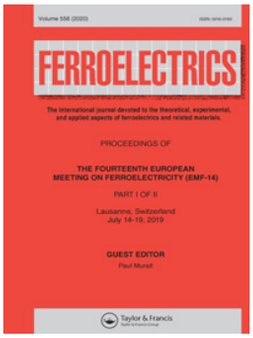

Ferroelectrics

ISSN: 0015-0193 (Print) 1563-5112 (Online) Journal homepage: https://www.tandfonline.com/loi/gfer20

Soft modes in $HoFe_{2.5}Ga_{0.5}(BO_3)_4$ solid solution

Alexander Krylov, Svetlana Krylova, Irina Gudim & Alexander Vtyurin

To cite this article: Alexander Krylov, Svetlana Krylova, Irina Gudim & Alexander Vtyurin (2020) Soft modes in $HoFe_{2.5}Ga_{0.5}(BO_3)_4$ solid solution, Ferroelectrics, 556:1, 16-22, DOI: 10.1080/00150193.2020.1713334

To link to this article: https://doi.org/10.1080/00150193.2020.1713334

Published online: 07 Apr 2020.

FERROELECTRICS
2020, VOL. 556, 16–22
https://doi.org/10.1080/00150193.2020.1713334

Taylor & Francis
Taylor & Francis Group

Soft modes in $HoFe_{2.5}Ga_{0.5}(BO_3)_4$ solid solution

Alexander Krylov[a], Svetlana Krylova[a], Irina Gudim[a], and Alexander Vtyurin[a,b]

[a]Kirensky Institute of Physics, FRC KSC SB RAS, Krasnoyarsk, Russia; [b]Siberian Federal University, Krasnoyarsk, Russia

ABSTRACT

The condensation of two soft modes has been found when studying the Raman spectra of the solid solution $HoFe_{2.5}Ga_{0.5}(BO_3)_4$ in the temperature range from 7 to 350 K. The first high-temperature soft mode is associated with the structural phase transition from the *R*32 phase to the $P3_121$ phase. The second soft mode is related to the reveal of the phonon-magnon interaction during magnetic ordering in the crystal. The temperatures of the structural phase transition $T_1 = 266$ K and the magnetic phase transition $T_2 = 28$ K are established. Experimentally interaction between the structural phase transition order parameter fluctuations and the magnetic order parameter fluctuations was found.

ARTICLE HISTORY
Received 14 July 2019
Accepted 24 December 2019

KEYWORDS
Soft modes; low temperatures; phonon-magnon interaction; magnetic ordering; huntite

1. Introduction

The $HoFe_{2.5}Ga_{0.5}(BO_3)_4$ solid solution belongs to the family of ferroborates with huntite structures. Most of the rare-earth ferroborates could be attributed to multiferroics [1–3]. In these materials at least two of several order parameters (electric, magnetic, elastic, etc.) coexist. Besides their coexistence, of utmost importance is a strong coupling between the two ferroic orders. In multiferroic materials, the coupling interaction between the different order parameters can produce additional functionalities. The application of multiferroics will enlarge the functional possibilities of spintronics significantly. The rare-earth ferroborates demonstrate a large variety of magnetic, magnetoelectric, magnetodielectric, and structural properties. $HoFe_3(BO_3)_4$ and $HoGa_3(BO_3)_4$ are prominent materials with an excellent perspective in multiferroic applications. The $HoFe_3(BO_3)_4$ crystal undergoes the phase transition at $T_c \approx 366$ K [4, 5]. Two magnetic phase transitions are found in the low-temperature region in $HoFe_3(BO_3)_4$ crystal. The transition from the paramagnetic to easy-plane antiferromagnetic state occurs at $T_N = 37.4$ K. The sharp heat capacity peaks and magnetization jumps are observed below 4.7 K. The $HoGa_3(BO_3)_4$ crystal exhibits a strong magnetoelectric effect [6]. The substitution compounds can provide an even wider variety of observed effects.

Currently, researchers actively study the structural and magnetic properties of solid solutions with other compositions by the Raman spectroscopy [7–10]. The soft modes and magnetic ordering were observed in all iron-containing systems.

CONTACT Alexander Krylov shusy@iph.krasn.ru
Color versions of one or more of the figures in the article can be found online at www.tandfonline.com/gfer.

In the present study, we consider the $HoFe_{2.5}Ga_{0.5}(BO_3)_4$ solid solution. Rare-earth ferroborates are characterized by an internal magnetic field induced by magnetic ordering below the temperature of the magnetic phase transition. The magnetic order will influence the Raman spectra also in absence of an external magnetic field. Low-frequency Raman spectroscopy is used as a tool in order to capture the soft mode frequency, which tends toward zero as the critical temperature is approached. Anomalous phonon softening under heating indicates the special role of phonons in crystal dynamics. Our work intends to observe such anomalies in Raman spectra connected with magnetic ordering and structural changes at low temperatures in the $HoFe_{2.5}Ga_{0.5}(BO_3)_4$ solid solution.

2. Experiment

Raman scattering spectra of $HoFe_{2.5}Ga_{0.5}(BO_3)_4$ has been studied in the temperature range from 8 K to 350 K. Raman spectra were collected in backscattering geometry, using a triple monochromator Jobin Yvon T64000 Raman spectrometer operating in double subtractive mode then detected by a liquid nitrogen-cooled CCD cooled at 140 K. The spectral resolution for the recorded Stokes side Raman spectra was better than $2\,cm^{-1}$ (this resolution was achieved by using gratings with 1800 grooves mm^{-1} and 100 μm slits). The spectral resolution of low-frequency region when soft mode investigated has been improved to $1.2\,cm^{-1}$ which attained a low- frequency limit of $10\,cm^{-1}$ in the present setup. The deformation of the low-frequency spectral edge by an optical slit, which sometimes smears the true features of the low-frequency spectra, was carefully eliminated by rigorous optical alignment. Single-mode argon 514.5 nm of Spectra-Physics Stabilite 2017 Ar^+ laser of 100 mW power (10 mW on the sample) was used as excitation light source.

The low-temperature experiments were carried out using a closed-cycle helium cryostat ARS CS204-X1.SS, controlled by LakeShore 340 temperature controller. The temperature was monitored by a calibrated silicon diode LakeShore DT- 670SD1.4L. Indium foil was used as a thermal interface. Measurements were taken inside the cryostat under pressure of 10^{-6} mBar. The above instrumentation allows to vary the sample cooling rate from 0.1 K/min up to 0.7 K/min with 0.1 K/min intervals.

The experiments were carried out in the dynamic regime by varying the sample temperature and it was identical to the measurement procedure at our past work [11]. The rates of temperature variation ranged were 0.7 K/min. The uncertainty of the measured temperature for a given rate can be estimated as a difference between adjacent measurements. The overall time for taking a single spectrum was within 30 s. The spectra were acquired with temperature steps of 0.7 K.

Experimental Raman spectra have been processed quantitatively using conventional damped harmonic oscillator (DHO) functions [12, 13]:

$$I(\omega) = F(\omega, T) \cdot \sum_i \frac{2A_i\omega_{0i}^2\gamma_i\omega}{\left(\omega_{0i}^2 - \omega^2\right)^2 + 4\gamma_i^2\omega^2}$$

where ω—current wavenumber, A, ω_0 and γ denote the intensity, harmonic wavenumber of the band center and full width at half maximum, respectively. The temperature factor $F(\omega, T)$ is calculated by

$$F(\omega, T) = \begin{cases} n(\omega) + 1 & Stokes \\ n(\omega) & Anti - Stokes \end{cases}$$

$$n(\omega) = \left[\exp\left(\frac{\hbar\omega}{k_B T}\right) - 1\right]^{-1}$$

with the Raman signal interplay between the Stokes and anti-Stokes parts near $0\,cm^{-1}$ uniquely obtained according to the temperature. $\hbar$, k_B is the reduced Planck constant and the Boltzmann constant respectively. The present Raman setup observes only the Stokes component. We used seven DHO functions for spectral fitting in the range of 10–300 cm^{-1}.

The samples under study were optically transparent, greenish single crystals with a size of about 3 mm and did not contain differently colored defects or inclusions visible under a microscope. The crystals were grown by the flux melt method and it is similar as described in previous works [9, 14].

3. Results and discussion

The $HoFe_3(BO_3)_4$ crystal belongs to space group $R32$ in the high-temperature phase. Under cooling, the crystal undergoes a structural phase transition, reducing the symmetry to $P3_121$. The number of Raman active modes is 26 for the high-temperature phase and 86 for the low-temperature phase. The symmetry analysis of the vibrational modes of the $R32$ structure of $HoFe_3(BO_3)_4$ is presented in Table 1. The one of the $P3_121$ structure is presented in Table 2.

The Raman spectra of $HoFe_{2.5}Ga_{0.5}(BO_3)_4$ solid solution should have some differences from the Raman spectra of $HoFe_3(BO_3)_4$, but we can expect a splitting of the E symmetry modes and the appearance of new modes under the sample cooling. The temperature spectra were obtained in parallel and crossed polarizers. The Raman signal maps are presented in Figure 1.

The maps clearly show that the sample is well oriented since the number of lines is different. The structural phase transition is visible from the figure. The appearance of new lines and a soft mode restoring below 270 K point to the structural phase

Table 1. Wyckoff positions and irreducible representations (Γ-point phonon modes) for $HoFe_3(BO_3)_4$ (Space group: $R32$, No. 155).

Atom space group: $R32$ (No. 155) Point group: $D3$		Wyckoff position	Γ-point phonon modes
Ho		3a	$A_2 + E$
Fe		9d	$A_1 + 2A_2 + 3E$
O		9e	$A_1 + 2A_2 + 3E$
O		9e	$A_1 + 2A_2 + 3E$
O		18f	$3A_1 + 3A_2 + 6E$
B		3b	$A_2 + E$
B		9e	$A_1 + 2A_2 + 3E$
Modes classifications			
Γ_{Raman}=$7A_1 + 19E$	$\Gamma_{IR} = 12A_2 + 19E$	$\Gamma_{ac} = A_2 + E$	$\Gamma_{Mehanical}$= $7A_1 + 13A_2 + 20E$
Raman tensor			

$$A_1 = \begin{bmatrix} a & 0 & 0 \\ 0 & a & 0 \\ 0 & 0 & b \end{bmatrix} \quad E(x) = \begin{bmatrix} c & 0 & 0 \\ 0 & -c & d \\ 0 & d & 0 \end{bmatrix} \quad E(y) = \begin{bmatrix} 0 & -c & -d \\ -c & 0 & 0 \\ -d & 0 & 0 \end{bmatrix}$$

Table 2. Wyckoff positions and irreducible representations (Γ-point phonon modes) for $HoFe_3(BO_3)_4$ (Space group: $P3_121$, No. 152).

Atom space group: $P3_121$ (No. 152) Point group: $D3$	Wyckoff position	Γ-point phonon modes
Ho	3a	$A_1 + 2A_2 + 3E$
Fe	6c	$3A_1 + 3A_2 + 6E$
Fe	3a	$A_1 + 2A_2 + 3E$
O	6c	$3A_1 + 3A_2 + 6E$
O	6c	$3A_1 + 3A_2 + 6E$
O	6c	$3A_1 + 3A_2 + 6E$
O	6c	$3A_1 + 3A_2 + 6E$
O	6c	$3A_1 + 3A_2 + 6E$
O	3b	$A_1 + 2A_2 + 3E$
O	3b	$A_1 + 2A_2 + 3E$
B	3b	$A_1 + 2A_2 + 3E$
B	6c	$3A_1 + 3A_2 + 6E$
B	3b	$A_1 + 2A_2 + 3E$
Modes classifications		
Γ_{Raman}=$27A_1 + 59E$ $\Gamma_{IR} = 32A_2 + 59E$	$\Gamma_{ac} = A_2 + E$	$\Gamma_{Mehanical}$= $27A_1 + 33A_2 + 60E$
Raman tensor		

$$A_1 = \begin{bmatrix} a & 0 & 0 \\ 0 & a & 0 \\ 0 & 0 & b \end{bmatrix} \quad E(x) = \begin{bmatrix} c & 0 & 0 \\ 0 & -c & d \\ 0 & d & 0 \end{bmatrix} \quad E(y) = \begin{bmatrix} 0 & -c & -d \\ -c & 0 & 0 \\ -d & 0 & 0 \end{bmatrix}$$

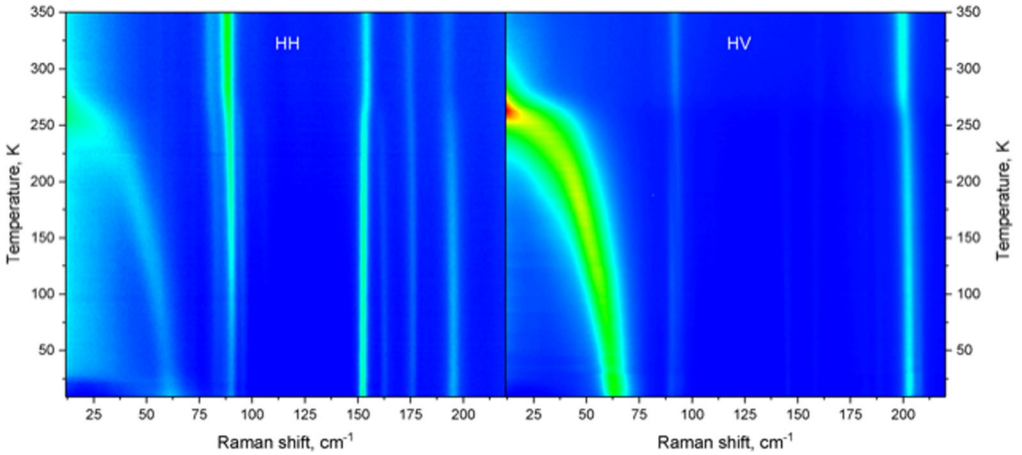

Figure 1. The Raman signal maps in the low-wavenumber part of the spectra in parallel and crossing polarizations.

transition. The soft mode connected with magnetic ordering is visible in the parallel polarization at temperatures lower than 30 K.

Three anomalies are seen clearly in Figure 2. The appearance of the new hard mode (90 cm^{-1}) below the temperature of the structural phase transition corresponds to the selection rules. The structural soft mode condensation from 7 cm^{-1} at 266 K to 65 cm^{-1} at 8 K have been observed. The restoration of the soft mode connected with magnetic ordering have been observed below 30 K. Two soft modes were also observed earlier in $Nd_xHo_{1-x}Fe_3(BO_3)_4$ solid solutions [14]. Their presence was associated with the coexistence of magnetic and structural order parameters.

We fitted this part of the spectrum using damped harmonic oscillator functions. The temperature dependence of reduced squared soft mode wavenumber $\omega_s^2 \equiv \omega^2 - \gamma^2$ is

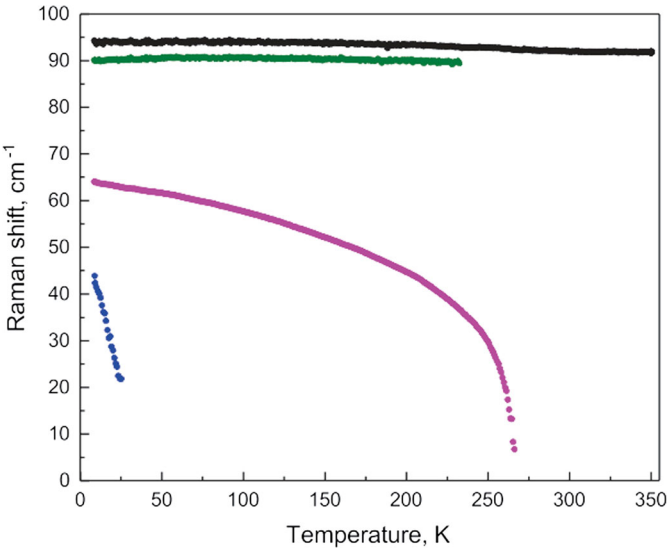

Figure 2. The mode positions dependence from the temperature in the low-wavenumber region.

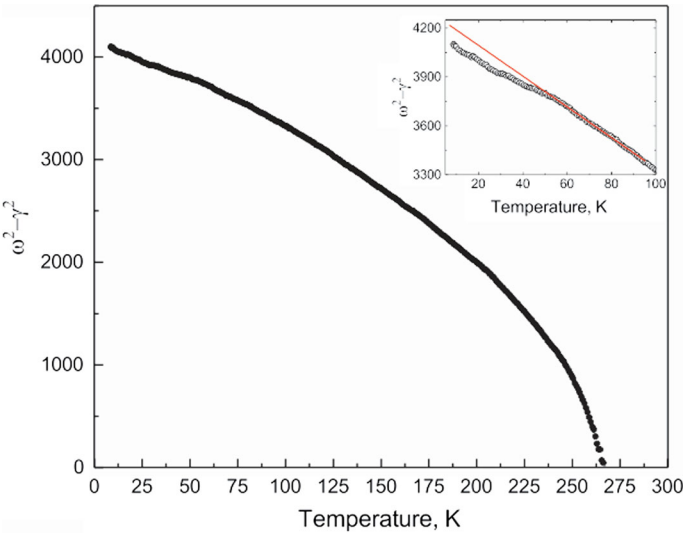

Figure 3. The reduced squared wavenumber of the structural soft mode vs. temperature.

typical for soft modes at the second order phase transition (Figure 3). However, we see an anomaly in the behavior of the soft mode below 50 K (top right corner in Figure 3). We attribute such change of the soft mode peak position below 50 K to the magnetoelastic interaction. It is the clear manifestation of the interaction between structural and the magnetic order parameters fluctuations. The estimated temperature of the structural phase transition is 266 K ($T_1 = 266$ K).

The temperature dependence of the squared wavenumber of the soft mode of magnetic ordering is presented in Figure 4. A linear approximation yields a Neel temperature at 28 K ($T_2 = 28$ K).

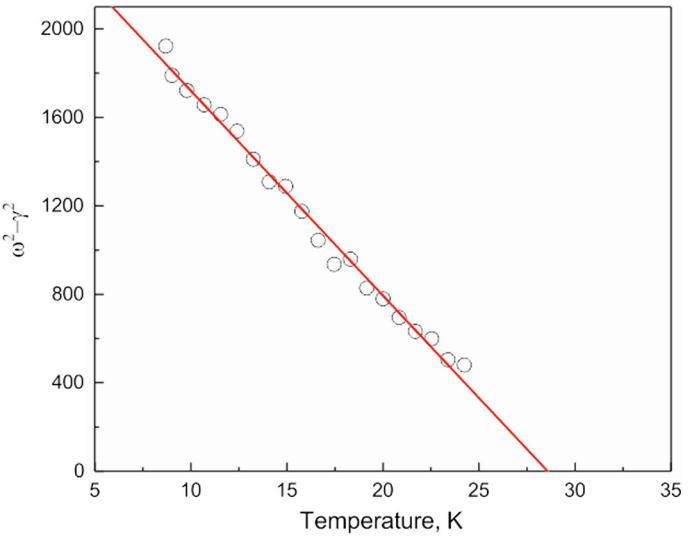

Figure 4. The squared wavenumber of the soft mode of magnetic ordering vs temperature. Linear approximation presented by the red line.

4. Conclusions

As a result of these investigations, we can conclude that the crystal $HoFe_{2.5}Ga_{0.5}(BO_3)_4$ undergoes a structural phase transition from the $R32$ phase to the $P3_121$ phase at $T_1 = 266$ K and that this transition is accompanied by a soft mode restoration. Another anomaly with a soft mode exists at $T_2 = 28$ K and corresponds to magnetic ordering.

The main changes in the spectra are observed in the low-wavenumber region (up to $100\,cm^{-1}$) where the mode related to magnetic ordering appears. A clear manifestation of the interaction between structural and magnetic order parameter fluctuations has been found.

Funding

This work was supported by the Russian Foundation for Basic Research Grant № 18-02-00754.

References

[1] J. F. Scott, Multiferroic memories, *Nat. Mater.* **6** (4), 256 (2007). DOI: 10.1038/nmat1868.
[2] M. M. Vopson, Fundamentals of multiferroic materials and their possible applications, *Crit. Rev. Solid State Mater. Sci.* **40** (4), 223 (2015). DOI: 10.1080/10408436.2014.992584.
[3] G. M. Kuz'micheva *et al.*, Crystallochemical design of huntite-family compounds, *Crystals*. **9** (2), 100 (2019). DOI: 10.3390/cryst9020100.
[4] A. Pankrats *et al.*, Low-temperature magnetic phase diagram of $HoFe_3(BO_3)_4$ holmium ferroborate: a magnetic and heat capacity study, *J. Phys: Condens. Matter*. **21**, 436001 (2009). DOI: 10.1088/0953-8984/21/43/436001.
[5] V. I. Zinenko *et al.*, Vibrational spectra and elastic, piezoelectric, and magnetoelectric properties of $HoFe_3(BO_3)_4$ and $HoAl_3(BO_3)_4$ crystals, *J. Exp. Theor. Phys.* **117** (6), 1032 (2013). DOI: 10.1134/S1063776113140203.

[6] N. V. Volkov *et al.*, Magnetization, magnetoelectric polarization, and specific heat of $HoGa_3(BO_3)_4$, *JETP Lett.* **99** (2), 67 (2014). DOI: 10.1134/S0021364014020106.

[7] D. Fausti *et al.*, Raman scattering from phonons and magnons in RFe3(BO3)4, *Phys. Rev. B.* **74** (2), 24403 (2006). DOI: 10.1103/PhysRevB.74.024403.

[8] A. Krylov *et al.*, Magnetoelastic interactions in Raman spectra of $Ho_{1-x}Nd_xFe_3(BO_3)_4$ crystals, *Solid State Commun.* **174**, 26 (2013). DOI: 10.1016/j.ssc.2013.09.011.

[9] E. Moshkina *et al.*, Crystal growth and Raman spectroscopy study of $Sm_{1-x}La_xFe_3(BO_3)_4$ ferroborates, *Cryst. Growth Des.* **16** (12), 6915 (2016). DOI: 10.1021/acs.cgd.6b01079.

[10] A. Krylov *et al.*, Low-temperature features of Raman spectra below magnetic transitions in multiferroic $Ho_{1-x}Nd_xFe_3(BO_3)_4$ and $Sm_{1-y}La_yFe_3(BO_3)_4$ single crystals, *Ferroelectrics.* **509** (1), 92 (2017). DOI: 10.1080/00150193.2017.1294040.

[11] A. Krylov *et al.*, Measurement of Raman-scattering spectra of $Rb_2KMoO_3F_3$ crystal: Evidence for controllable disorder in the lattice structure, *Cryst. Growth Des.* **14** (3), 923 (2014). DOI: 10.1021/cg4008894.

[12] H. Taniguchi, M. Itoh, and D. Fu, Raman scattering study of the soft mode in $Pb(Mg_{1/3}Nb_{2/3})O_3$, *J. Raman Spectrosc.* **42** (4), 706 (2011). DOI: 10.1002/jrs.2746.

[13] A. S. Krylov *et al.*, Structural transformations in a single-crystal Rb_2NaYF_6: Raman scattering study, *J. Raman Spectrosc.* **44** (5), 763 (2013). DOI: 10.1002/jrs.4263.

[14] A. S. Krylov *et al.*, N. Manifestation of magnetoelastic interactions in Raman spectra of $Ho_xNd_{1-x}Fe_3(BO_3)_4$ crystals, *J. Adv. Dielectrics.* **8** (2), 850011 (2018).